

発電用マイクロレシプロエンジンの設計

正員 杉山 進* 正員 鳥山 寿之**

Design of a Micro Reciprocating Engine for Power Generation

Susumu Sugiyama*, Member, Toshiyuki Toriyama**, Member

A reciprocating engine was designed for a micro power generator. It is expected to be used for a portable micro power generator with high energy density. The proposed reciprocating engine has the spring system, which is composed of opposite-pistons supported by an elastic spring. Combination of resonance of the spring system by the combustion pressure and an induction coil generates electricity due to generated voltage. Working cycle analysis, structural analysis, vibration analysis, and generated voltage calculations were carried out. Adopting H_2 gas as a fuel and Si as a structural material, the theoretical output was found to be 41 mW under the conditions that compression ratio is 5, the maximum combustion temperature is 850 K and resonance frequency of the spring system is 582 Hz.

キーワード：レシプロエンジン、マイクロ発電機、オットーサイクル、共振

Keywords: reciprocating engine, micro power generator, Otto cycle, resonance

1. Introduction

Recently, in the field of power generation, a small and distributed power generation system, which supports the individual power generation by consumers, has been progressed in place of the conventional large-scale systems. Especially, in the field of small energy sources used for portable equipments, small batteries are widely used. However, their energy density is relatively low, and they do not always satisfy the desired performance⁽¹⁾. On the other hand, miniaturization of heat engine by MEMS technology, which is expected to realize high energy density, has been proposed since middle of '90s. Since, Epstein *et al.*⁽²⁾ began to develop a micro turbine for portable micro power generator, several researches for micro turbines were reported⁽³⁾⁽⁴⁾. Park *et al.*⁽⁵⁾ have begun to develop micro piston engines, i.e., reciprocating engines.

In this paper, structure, performance and power generation mechanism of a reciprocating engine were designed for a micro power generator. The proposed micro power generator has the spring system, which is composed of opposite-pistons supported by an elastic spring. Power generation mechanism is based on the generated voltage induced by power generation system composed of permanent magnets and induction coils, which are located on the piston terminals and outside of the engine. The resonance of the spring system due to combustion pressure can be used to increase the generated voltage generation in the power generation system.

2. Structural Concept

The proposed reciprocating engine-type micro power generator hereafter, we call micro power generator, is composed of an engine part where the chemical energy changes into the mechanical energy through the thermal energy and a generator part where the mechanical energy changes into the electric energy.

The schematic view of structural concept is shown in Fig. 1. The typical dimensions of the engine parts are shown in Fig. 2. The clearance between the piston and the cylinder case is set to 3 μm , depending on the tolerance of photolithography process. The main structural material for the engine part is Si.

The engine part is composed of opposite-pistons, an elastic spring, a cylinder case, and a top glass plate. The opposite-pistons are reciprocated by receiving impact force due to the combustion. The elastic spring supports the pistons and

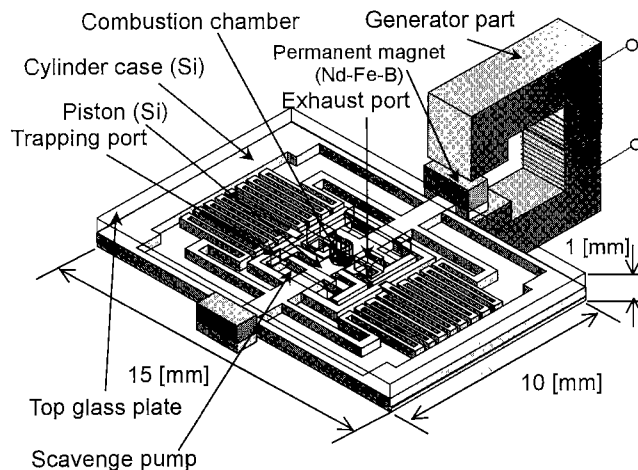


Fig. 1. Concept of proposed reciprocating engine.

* 立命館大学 理工学部
〒525-8577 滋賀県草津市野路東 1-1-1
Faculty of Science and Engineering, Ritsumeikan University
1-1-1 Noji-Higashi, Kusatsu, Shiga 525-8577

** 立命館大学 COE 推進機構
〒525-8577 滋賀県草津市野路東 1-1-1
Center for promotion of the COE program, Ritsumeikan University
1-1-1 Noji-Higashi, Kusatsu, Shiga 525-8577

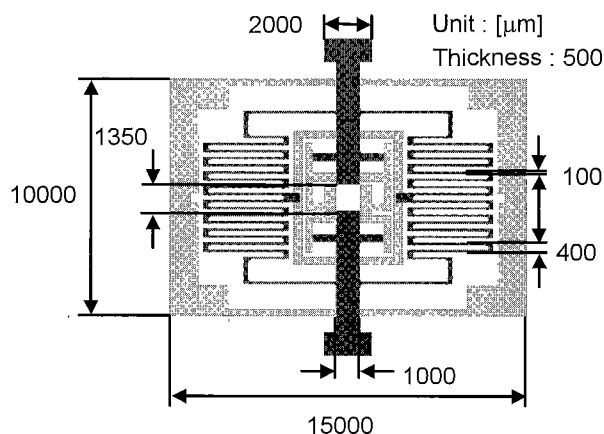


Fig. 2. Typical dimensions of the engine.

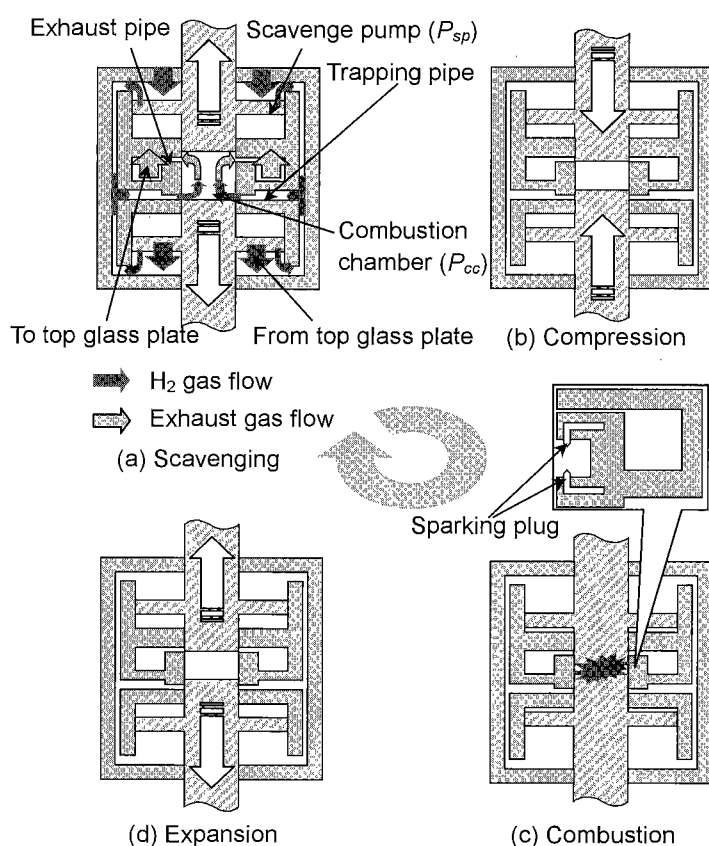


Fig. 3. Two-stroke cycle.

composes the spring system. The cylinder case guides the movement of the pistons and has a trapping pipe, an exhaust pipe, and a scavenge pump.

The top glass plate is fixed on the surface of the cylinder case and has a trapping port and an exhaust port. As shown in Fig. 3, we adopt the two-stroke cycle as a working cycle of the micro power generator. In case of the two-stroke cycle engine, cycle reciprocation of the piston occurs per combustion. Whereas, in case of the four-stroke cycle engine, two cycle reciprocations of the piston occur per combustion. Therefore, there is an advantage in the two-stroke cycle engine that it has larger specific power, i.e., energy - density / weight than the four-stroke cycle engine. As shown in Fig. 3(a), pressure

difference between the combustion chamber (P_{cc}) and the scavenge pump (P_{sp}), i.e., $P_{sp} > P_{cc}$ can be used for the scavenging. The scavenge pump is necessary for the trapping - exhaust exchange, and it realizes piston-piston scavenging, i.e., uniflow scavenging by the opposite-pistons. Ignition is done by a sparking plug. Transformer-induced high voltage acts on the sparking plug.

The generator part of the reciprocating engine-type micro power generator is composed of a coil around the iron core having a gap (Fig. 1). It is located externally to the engine. The permanent magnet, which is fixed on the piston terminal, reciprocates through the gap of the coil. This motion induces generated voltage due to a magnetic flux change, i.e., Faraday - Lentz electromagnetic induction.

3. Design

Design is classified into three items as follows. (I) The working cycle design, which is based on the Otto cycle. (II) The vibration analysis of the piston against the combustion pressure. The modal analysis and the stress analysis of the piston and elastic spring, the heat transfer and radiation analysis of the engine structure. (III) The calculation of the induced generated voltage based on the equivalent magnetic circuit model of the generator.

3.1 Working Cycle The Otto cycle was adapted for the working cycle design. The quenching distance and the combustion velocity of gas contribute for the down sizing of the engine system. Therefore, we adopt the hydrogen gas having excellent characteristics against above-mentioned properties⁽⁶⁾. In the Otto cycle, theoretical thermal efficiency η_v is determined by the compression ratio ε and the specific heat ratio κ as⁽⁶⁾,

$$\eta_v = 1 - \frac{1}{\varepsilon^{\kappa-1}} \quad (1)$$

According to Eq. (1), the theoretical thermal efficiency is independent of the amount of heat supply, and increases with increasing the compression ratio. In case of a higher compression ratio, the knock occurs during the compression stroke by the spontaneous ignition, and decreases the thermal efficiency. Therefore, in the Otto cycle, a compression ratio of less than 11 is usually adopted. Taking into account of this, the micro power generator adopts a compression ratio of 5 as prototyping. In case of constant stroke volume, i.e., $V_H = \text{constant}$, higher combustion temperature (T_3) leads to higher combustion pressure (P_3), and consequently higher output power⁽⁶⁾,

$$\frac{P_3}{P_1} = \varepsilon \frac{T_3}{T_1} \quad (2)$$

where, T_1 is ambient temperature, and P_1 is ambient pressure. However, the permissible temperature of the structural material for the engine part restricts the upper limit of the combustion temperature.

Therefore, the structural material of the micro power generator must have characteristics of high strength and low thermal expansion coefficient under intermediate temperature range. The structural material must be easy to process by the

Table 1. Data for calculation of engine performance ⁽⁶⁾

Stroke volume V_H [m^3]	5.00×10^{-10}
Compression ratio ε	5.00
Indicated thermal efficiencies η_g	0.55
Minimum air quantity L_{min} [m^3/kg]	2.38
Air-excess factor λ	8.08
Lower calorific value of fuel H_u [J/kg]	108×10^5
Specific heat ratio κ [$\text{J}/(\text{kg K})$]	1.41
Theoretical thermal efficiency η_v	0.22

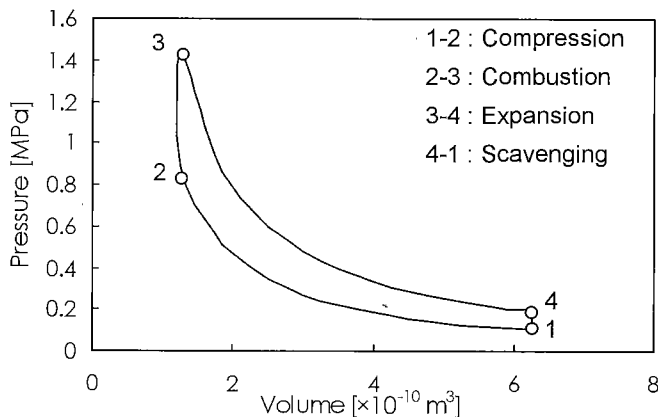


Fig. 4. Pressure - volume diagram.

MEMS technology. Taking into account these things, we adopt Si as the structural material for the engine part.

Some fundamental parameters, which can be used to determine the pressure - volume diagram of the Otto cycle, are given in Table 1. Using Table 1 and fundamental working cycle analysis of the Otto cycle ⁽⁶⁾, the pressure - volume diagram can be obtained as Fig. 4.

3.2 Structural and Vibration Analysis In the MEMS field, as can be seen in the mechanical sensors, the resonance of the structure can be used for driving and sensing. In order to increase the relative output power of the micro power generator; a constant period combustion is used to resonate the piston, i.e., to increase displacement and speed of the piston.

In order to examine the influence of the frequency ratio (f_i/f_n) on the maximum amplitude of vibration, the vibration of the spring system was analyzed. Where f_n is the natural frequency of the spring system composed of the pistons and elastic spring, and f_i is the frequency of ignition period. As shown in Fig. 5, it is assumed that the spring system can be modeled as a one degree of freedom linear vibration system and the impact power due to the combustion pressure can be modeled as a semi-sine wave pulse. The one-degree of freedom linear vibration induced by the semi-sine wave pulse is expressed by the following equations ⁽⁷⁾,

$$m\ddot{x}(t) + c\dot{x}(t) + kx(t) = F(t) \quad (3)$$

$$F(t) = F \sin(2\pi f_c t) \quad (0 < t < t_c), \quad (4)$$

$$F(t) = 0 \quad (t > t_c), \quad (5)$$

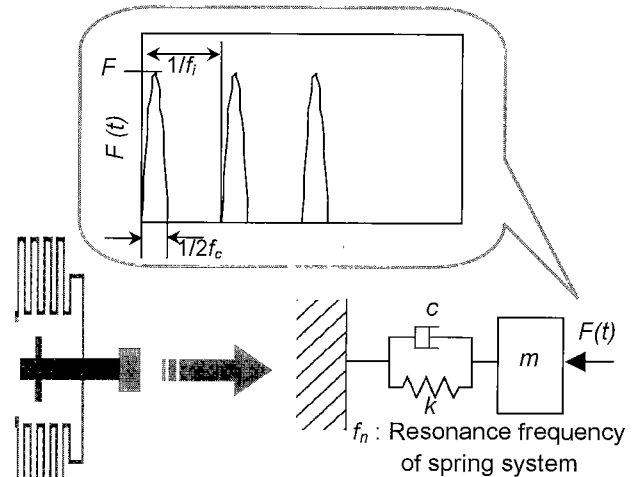


Fig. 5. One degree of freedom linear vibration system and semi-sine wave pulse.

where, m is mass of the spring system, x is displacement of the piston, c is equivalent viscosity attenuation coefficient, k is equivalent spring constant, F is impact power, f_c is frequency of the semi-sine wave pulse, t is time, and t_c is $1/2f_c$, respectively. In the equations, the time interval of the impact pulse response corresponds to $0 < t < t_c$, and that of the natural vibration corresponds to $t_c < t$.

In order to determine the equivalent spring constant k and the natural frequency f_n (Eqs. (3) and (5)) of the spring system, FEM analysis was carried out using MEMCAD4. In the analysis, displacement in the X direction (transverse direction of the piston) is fixed, because the piston is guided along the cylinder case and restricted to move to Y direction (longitudinal direction) only. The result of FEM stress analysis of the spring system is shown in Fig. 6. The result of FEM modal analysis of the spring system is shown in Fig. 7. From Fig. 6, the displacement of the spring system is $1021 \mu\text{m}$ under pressure of 1 MPa. In this case, the maximum Mises stress is 648 MPa, and located in the connection part between the piston and the spring. This value is lower than the fracture strength of Si ($\sim 1 \text{ GPa}$) ⁽⁸⁾. From Fig. 7, the 1st, the 2nd and the 3rd natural frequencies of the spring system are 582 Hz, 3119 Hz and 3183 Hz, respectively. Comparing to the analysis of Eqs. (3) and (5), i.e., impact pulse response, based on the standard FEM is difficult. Therefore, an explicit analysis was carried out in this case.

Figure 8(a) and 8(b) show examples of vibration of the piston in case of $f_i/f_n = 0.50$ and $f_i/f_n = 1.05$, respectively. In the analysis, it is assumed that the semi-sine wave pulse of frequency f_c is applied to the spring system under interval of frequency f_i . The f_i is equivalent to the frequency of the ignition period (see Fig. 5). The viscosity attenuation coefficient is assumed to be $\zeta = c / (4\pi m f_n) = 0.2$. The impact power F can be calculated from the cross product of the combustion pressure P_3 in Fig. 4 and cross sectional area of the piston. The frequency of the semi-sine wave pulse f_c can be calculated as an inverse of combustion interval of H_2 gas. In Fig. 8, the solid line shows the impact pulse response region and the dotted line shows the

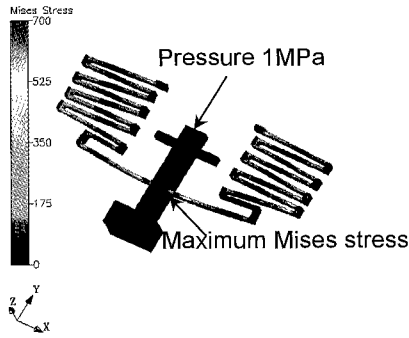


Fig. 6. FEM stress analysis of piston.

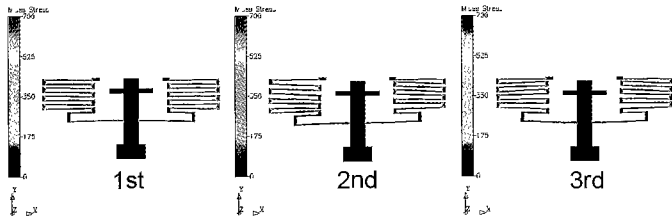


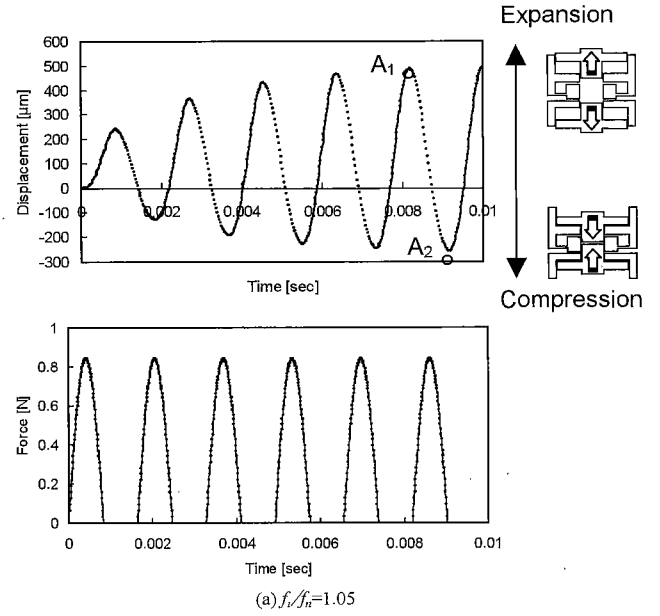
Fig. 7. FEM modal analysis of piston.

natural vibration region.

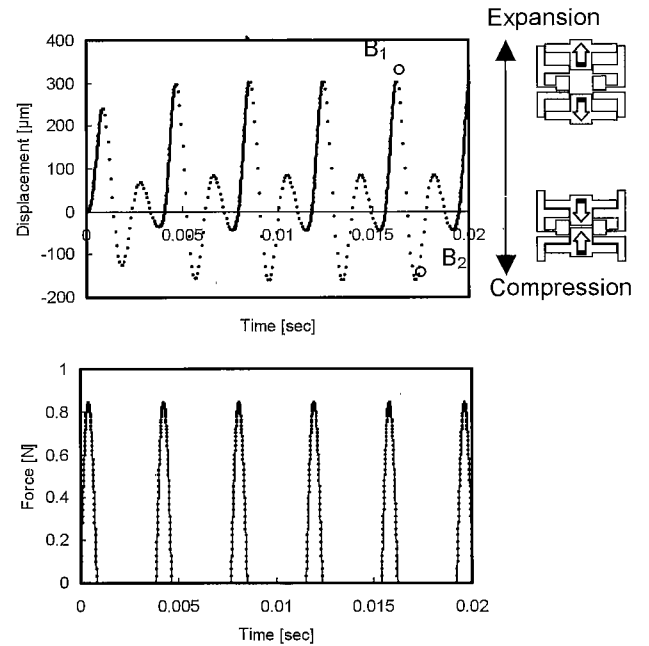
In the case of $f_i/f_n = 0.50$ and 1.05 , the maximum displacements under the expansion stroke correspond to A_1 and B_1 , respectively. On the other hand, the maximum displacements under compression stroke correspond to A_2 and B_2 , respectively. As shown in Fig. 8(a), steady-state vibration, which is the alternation of expansion by the impact pulse response and the compression by the natural vibration, was obtained. This can be achieved by setting the frequency f_i (610 Hz) of ignition period close to the 1st natural frequency f_n (582 Hz) of the spring system. On the other hand, as shown in Fig. 8(b), unstable vibration, which is the alternation of expansion by the impact pulse response and series of compression - expansion - compression cycle by the natural vibration, was obtained. This is due to the adoption of the frequency f_i (291 Hz) to be half of the frequency f_n .

As previously mentioned, we adopt the two-stroke cycle, where the piston reciprocates one cycle per combustion. Therefore, the vibration of the neighborhood of $f_i/f_n = 1$ where the one cycle reciprocation per combustion can be achieved, is most suitable for our purpose. Figure 8(c) shows the change of the maximum displacement of the piston under the expansion stroke and the compression stroke with the variation of f_i/f_n . In Fig. 8(c), the maximum displacement can be obtained in the case of $f_i/f_n = 1$. However, in this case, the maximum stress in the spring system is larger than fracture strength of Si. Therefore, we adopt the vibration in the neighborhood of $f_i/f_n = 1$, except for $f_i/f_n = 1$.

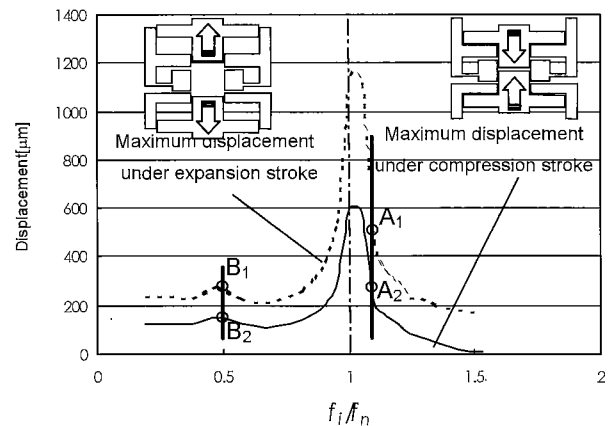
In the case of $f_i/f_n < 1$, the impact pulse response is finished after the piston changes position from the expansion to the compression process (see lower figure in Fig. 8(b)). In the case of $f_i/f_n > 1$, the impact pulse response is finished before the piston changes position from the expansion to the compression process (see lower figure in Fig. 8(a)). Therefore, in order to



(a) $f_i/f_n = 1.05$



(b) $f_i/f_n = 0.50$



(c) Change of the maximum displacement

Fig. 8. Vibration analysis.

realize the smooth reciprocation of the piston with the impact power, we must choose $f_i/f_n > 1$, i.e., $f_i/f_n = 1.05$ in the design.

In order to determine the thermal expansion and the thermal stress of the cylinder case due to the heat transfer from the combustion chamber, FEM analysis was carried out. The temperature distribution, the thermal stress, the thermal deformation were analyzed under the condition that wall temperature of the combustion chamber 850 K corresponding to the design value of T_{max} in the working cycle design. The analysis is steady state and does not take into account the convection such as the exhaust heat. As shown in Fig. 9, the average temperature is 512 K. This temperature is lower than creep temperature of Si (673 K)⁽⁹⁾. The maximum thermal stresses are 24.3 MPa, and lower than the fracture strength of Si less than 512 K⁽⁸⁾. The maximum thermal deformation along the perpendicular direction to the motion of the piston (the direction of the X) is 0.04 μm . This value is sufficiently small

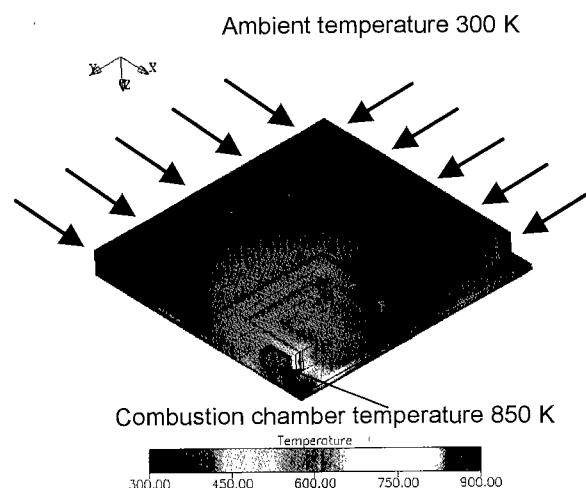


Fig. 9. FEM thermal analysis of cylinder case.

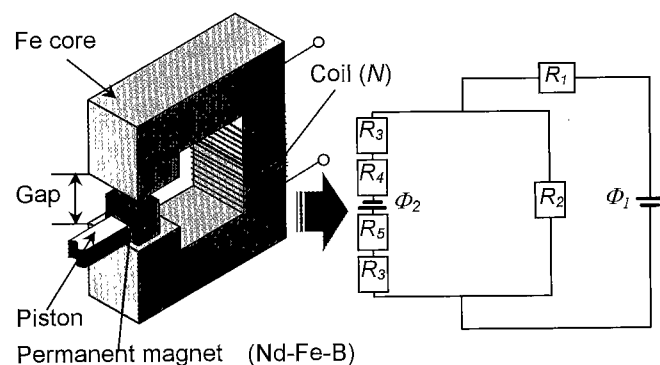


Fig. 10. Equivalent magnetic circuit of the generator.

(*) In this case, the viscosity attenuation coefficient is assumed to be $\zeta = c / (4\pi m f_n) = 0.2$ as previously mentioned. If $\zeta = 0.1$, the resultant output power is increasing and found to be $\sim 68 \text{ mW}$. However, if ζ is more than ~ 0.7 , the resonance, i.e., increment of the piston displacement does not occur in this vibration system, and the resultant output power is found to be $\sim 14 \text{ mW}$ ⁽⁷⁾. Therefore, some tries and errors in the engine structure may be necessary to derive the ζ less than ~ 0.2 by experiment.

compared with the clearance between the piston and cylinder case, i.e., 3 μm , and does not influence the air leakage and motion of the piston.

3.3 Output Power Calculation An equivalent magnetic circuit of the generator is shown in Fig. 10. The induced generated voltage due to the flux change in the coil can be analyzed. Magnetic flux Φ_1 in the iron core and induced generated voltage V are given by⁽¹⁰⁾

$$\Phi_1 = \frac{R_2 R_4 \Phi_2}{(R_1 + R_2)(R_2 + 2R_3 + R_5) - R_2^2}, \quad (6)$$

$$V = -N \frac{\partial \Phi_1}{\partial t}, \quad (7)$$

where, R_1 is reluctance of iron core, R_2 is reluctance of gap, R_3 is reluctance of space between permanent magnet and iron core or between piston and iron core, R_4 is reluctance of permanent magnet, R_5 is reluctance of piston, Φ_2 is magnetic flux of permanent magnet, and N is number of turns of the coil, respectively. The reluctance $R_1 \sim R_5$ are function of shape of the coil (see Fig. 10) and depending on the vibration mode of the spring system^(*). The vibration mode in Fig. 8(a) can be used for the calculation of $R_1 \sim R_5$. Φ_2 is determined by the property of the permanent magnet (Nd-Fe-B). $N = 500$ is adopted. As a result, the generated voltage V was found to be 26 mV and corresponding output power is 41 mW.

4. Conclusions

Structure and performance of a reciprocating engine was designed for a micro power generator. Working cycle analysis, structural analysis, vibration analysis, and generated voltage calculation were carried out. Adopting H_2 gas as a fuel and Si as a structural material, the theoretical output power was found to be 41 mW under the conditions that compression ratio is 5, the maximum combustion temperature is 850 K, and natural frequency of the spring system is 582 Hz.

As a further work, fabrication process of the reciprocating engine-type micro power generator will be completed. Through the performance evaluation, the validity of the design must be confirmed.

Acknowledgment

The authors would like to thank S. Nakano and K. Hashimoto at Ritsumeikan University for their help with numerical simulations and preparing figures.

(Manuscript received Jun. 1, 2003, revised April 18, 2003)

References

- (1) S. Tanaka : "New Development of Power Sources for Portable Devices", *Journal of the Japan Society of Mechanical Engineers*, Vol.105, pp.35-39 (2002) (in Japanese)
- (2) A.H. Epstein : "Power MEMS and Microengines", *Transducers'97*, Vol.2, pp.753-756 (1997)
- (3) M.A. Schmit : "Technologies for Micro Turbo Machinery", *Transducers'01*, Vol.1, pp.2-5 (2001)
- (4) S. Tanaka : "Air-turbine-driven Micro-polarization Modulator for Fourier Transform Infrared Spectroscopy", *Technical Digest of The 17th Sensor Symposium*, pp.29-32 (2000)
- (5) D.E. Park : "Design and Fabrication of Micromachined Internal

Combustion Engine as a Power Source for Microsystems", *MEMS2002*, pp 272-275 (2002)

- (6) H. Yanagihara : *Verbrennungskraftmaschinen* : Herausgegeben von Rikogakusha Publishing Co. (2000) (in Japanese)
- (7) JSME Mechanical Engineers' Handbook A Fundamentals A3 Mechanics and Mechanical Vibrations (1986) (in Japanese)
- (8) S. Johansson : "Fracture testing of silicon microelements *in situ* in a scanning electron microscope", *J. Appl. Phys.*, Vol. 63, pp. 4799-4803 (1988)
- (9) G.L. Pearson : "Deformation and fracture of small silicon crystals," *Acta Metallurgica*, Vol. 5, pp. 181-191 (1957)
- (10) K. Okawa : *An Introduction of Permanent Magnet Magnetic Circuit*, Sogodenshisuppansha (1994) (in Japanese)

Susumu Sugiyama (Member) received the B.S. degree in Electrical Engineering from Meijo University, Nagoya, in 1970, and the Dr. E. degree from Tokyo Institute of Technology, Japan, in 1994. From 1965 to 1995, he was with Toyota Central Research & Development Laboratories, Inc., where he worked on semiconductor strain gages, silicon pressure sensors, integrated sensors and micromachining. While there, he was a Senior Researcher, Manager of the Silicon Devices Laboratory, and Manager of the Device Development Laboratory. Since 1995 he has been with Ritsumeikan University, Shiga, Japan, where he recently serves as a Professor in the Department of Robotics, Faculty of Science and Engineering. He is Editor-in-Chief of *Sensors and Materials*. His current interests are microsensors and microactuators and high aspect ratio micro structure technology.



Toshiyuki Toriyama (Member) received the Ph.D. degree in 1994 from Kyushu University, Fukuoka, Japan. He is currently an Associate Professor in the Center for Promotion of the COE Program of Ritsumeikan University. His current interests are piezoresistive mechanical sensors and MEMS heat engines.

